Atmos. Meas. Tech. Discuss., 7, 819–858, 2014
www.atmos-meas-tech-discuss.net/7/819/2014/
doi:10.5194/amtd-7-819-2014

Atmospheric Measurement Techniques Discussions
Open Access

Characterisation of an inlet pre-injector laser induced fluorescence instrument for the measurement of ambient hydroxyl radicals

A. Novelli[1], K. Hens[1], C. Tatum Ernest[1], D. Kubistin[1,*], E. Regelin[1], T. Elste[2], C. Plass-Dülmer[2], M. Martinez[1], J. Lelieveld[1], and H. Harder[1]

[1]Dept. Airchemistry, Max Planck Institute for Chemistry, 55128 Mainz, Germany
[2]German Weather Service, Meteorological Observatory Hohenpeissenberg (MOHp), Albin-Schwaiger-Weg 10, 83282 Hohenpeissenberg, Germany
[*]now at: University of Wollongong, School of Chemistry, Wollongong, NSW, Australia

Received: 8 January 2014 – Accepted: 16 January 2014 – Published: 28 January 2014

Correspondence to: H. Harder (hartwig.harder@mpic.de)

Published by Copernicus Publications on behalf of the European Geosciences Union.

Abstract

Ambient measurements of hydroxyl radicals (OH) are challenging due to a high reactivity and consequently low concentration. The importance of OH as an atmospheric oxidant has resulted in a sustained effort leading to the development of a number of analytical techniques. Recent work has indicated that the laser-induced fluorescence of the OH molecules method based on the fluorescence assay by gas expansion technique (LIF-FAGE) for the measurement of atmospheric OH in some environments may be influenced by artificial OH generated within the instrument, and a chemical method to remove this interference was implemented in a LIF-FAGE system by Mao et al. (2012). We have applied this method to our LIF-FAGE HORUS (HydrOxyl Radical Measurement Unit based on fluorescence Spectroscopy) system, and developed and deployed an inlet pre-injector (IPI) to determine the chemical zero level in the instrument via scavenging the ambient OH radical.

We describe and characterise this technique in addition to its application at field sites in forested locations in Finland, Spain, and Germany. Ambient measurements show that OH generated within the HORUS instrument is a non-negligible fraction of the total OH signal, which can comprise 30 % to 80 % during the day and 60 % to 100 % during the night. The contribution of the background OH varied greatly between measurement sites and was likely related to the type and concentration of volatile organic compounds (VOCs) present at each particular location. Two inter-comparisons in contrasting environments between the HORUS instrument and two different chemical ionisation mass spectrometers (CIMS) are described to demonstrate the efficacy of the inlet-pre-injector and the necessity of the chemical zeroing method in such environments.

1 Introduction

The hydroxyl radical, OH, plays a central role in the chemistry of the troposphere, where it acts as the main daytime oxidizing agent, initiating the photochemical degradation of many chemical species emitted by natural and anthropogenic sources. In the lower troposphere the OH radical is primarily produced by photolysis of ozone and subsequent reaction of the excited oxygen atom with water vapour (Levy, 1971). Minor primary sources are the photolysis of nitrous acid and hydrogen peroxide and ozonolysis of unsaturated compounds. Once formed, the OH radical reacts rapidly with many atmospheric trace gas species converting more than 90 % of the volatile organic matter (Levy, 1974). The ambient measurement of OH is therefore a good test of proposed chemical mechanisms postulating the importance of chemical species and/or processes in the atmosphere. The OH radical is usually measured in the field with one of three techniques: differential optical absorption spectroscopy (DOAS) (Perner et al., 1987) via absorption of light by OH, chemical ionization mass spectrometry (CIMS) (Eisele and Tanner, 1991) via the detection of H_2SO_4 after the oxidation of SO_2 by atmospheric OH, and laser-induced fluorescence (LIF-FAGE) (Hard et al., 1984) via the detection of OH radical fluorescence after laser excitation. Several comparison campaigns have been performed, both on ground (Hofzumahaus et al., 1998; Schlosser et al., 2007) and aircraft (Eisele et al., 2001; Ren et al., 2012), in order to test the consistency and performance of the different techniques and have generally shown good agreement. However, a number of recent measurements performed by LIF-FAGE instruments in VOC rich environments have shown considerably higher values of OH radicals than can be accounted for by well established chemical mechanisms (Faloona et al., 2001; Lelieveld et al., 2008; Ren et al., 2008; Hofzumahaus et al., 2009; Kubistin et al., 2010; Whalley et al., 2011). These model-measurement disagreements have prompted the discovery of new chemical paths (Dillon and Crowley, 2008; Peeters et al., 2009; da Silva, 2010a, b, c; Crounse et al., 2011) and the development of alternative chemical mechanisms to account for the discrepancies (Lelieveld et al., 2008; Hofzumahaus et al., 2009; Peeters et al., 2009; Peeters and Müller, 2010; Taraborrelli et al., 2012). At least in part, responsibility for the disagreement between models and measurements could lie on the side of the measurement technique. LIF instruments can suffer from a number of well characterised interferences, such as OH generated by the laser pulse from species like ozone, acetone, or H_2O_2, as well as spectral interferences from, for example, naphthalene and SO_2. When present, these can be corrected for (Holland and Hessling, 1995; Martinez et al., 2004; Ren et al., 2004; Kubistin, 2009). Recent work by Mao et al. (2012) suggested that, at least in some LIF-FAGE designs and possibly depending on the characteristics of the environment, a process not currently accounted for may generate OH within the low pressure side of the instrument. The authors report the measurement of OH radicals in a Ponderosa pine plantation in the California Sierra Nevada Mountains with the deployment of a chemical zero level system in parallel with the traditional FAGE method.

In this paper, we describe the characterisation and application of such a chemical zero system (inlet pre-injector, IPI) to the HORUS instrument, following the design in Mao et al. (2012), to address the possible role of internally-formed OH in our system. In addition, we also describe how the atmospheric OH concentration is determined with the new modification of the instrument in three field measurements which include two comparisons of the Mainz IPI-LIF-FAGE instrument with CIMS measurements of OH in chemically distinct environments.

2 Methodology

2.1 Mainz LIF-FAGE description

The LIF-FAGE instrument (HORUS) in use at the Max Planck Institute for Chemistry, Mainz, is based on the design of GTHOS (Ground Tropospheric Hydrogen Oxide Sensor) described by Faloona et al. (2004) and is described in detail by Martinez et al. (2010). The instrument consists of three parts: the inlet and detection system, the laser system, and the vacuum system (Fig. 1). The air is drawn at ~ 7 $\mathrm{L\,min^{-1}}$ through a critical orifice (1 mm diameter) and OH is selectively excited by pulsed UV light at around 308 nm on resonance with the $Q_1(2)$ transition line ($A^2\Sigma^+ - X^2\Pi$, $v' = 0$, $v'' = 0$). The laser pulse is directed into a multipass "White Cell" (White, 1942) crossing the detection volume 32 times to increase the sensitivity. The fluorescence signal from the excited hydroxyl radicals is detected at low pressure (∼ 300–500 Pa). As the fluorescence is detected at similar wavelengths as the excitation one, a time-gated photon counting technique using micro-channel plate detectors (MCP) is used. The UV light for excitation of the hydroxyl radicals is provided by a Nd:YAG pumped, pulsed, tunable dye laser system (Wennberg et al., 1994; Martinez et al., 2010) operated at a pulse repetition frequency of 3 kHz. The instrument has two consecutive detection cells: in the first cell OH radicals are detected, and in the second cell hydroperoxyl radicals (HO_2) are detected via the conversion of HO_2 to OH by the addition of NO. The calibration of the instrument is achieved via production of a known amount of OH and HO_2 from the photolysis of water at 185 nm using a mercury lamp. A more detailed description of the instrument calibration is reported by Martinez et al. (2010). The fluorescence background signal of the instrument is measured by tuning the excitation laser on (online signal, $\mathrm{Sig}^{\mathrm{on}}$) and off (offline signal, $\mathrm{Sig}^{\mathrm{off}}$) resonance with the OH transition line at 308 nm (Fig. 2a). The spectra of the measured atmospheric OH is compared with the one obtained from a reference cell in order to rule out possible fluorescence signal due to species that fluoresce at similar wavelengths (such as naphthalene and SO_2).

2.2 Inlet Pre-Injector (IPI)

Figure 3 shows a schematic cross-section of IPI currently in use as part of the HORUS instrument. The purpose of IPI is the addition of an OH scavenger to remove the atmospheric OH before it is sampled by the inlet in order to account for an OH signal generated within the instrument. Before the introduction of IPI, the atmospheric OH concentration was obtained by multiplying the OH fluorescence signal (OHF), obtained from the difference between fluorescence online and fluorescence offline signals, by the total instrument sensitivity (S). The total instrument sensitivity depends on many parameters such as laser power, efficiency of the detector, temperature and, humidity

(Martinez et al., 2004) and is determined by performing calibrations on a regular basis.

$$\mathrm{OHF} = (\mathrm{Sig}^{\mathrm{on}} - \mathrm{Sig}^{\mathrm{off}}) \tag{1}$$

$$\mathrm{OH} = S \times \mathrm{OHF} \tag{2}$$

With IPI (Fig. 2b), the instrument is also cycled every 2 min between injection of the scavenger (background OH fluorescence signal detected, $\mathrm{OHF_{bg}}$) and no injection (total OH fluorescence signal detected, $\mathrm{OHF_{tot}}$). The atmospheric OH concentration ($\mathrm{OH_{atm}}$) is then obtained by multiplying the difference between the total OH fluorescence signal and the background OH fluorescence signal by the instrument sensitivity and by a factor (F) accounting for scavenging efficiency and radical losses introduced by IPI.

$$\mathrm{OH_{atm}} = (S \times (\mathrm{OHF_{tot}} - \mathrm{OHF_{bg}})) \times F \tag{3}$$

To compare the derived atmospheric OH concentration with the respective total and background signals and to describe the error in concentration of atmospheric OH that would have been made without the use of IPI, we apply the same OH calibration factor to both OH fluorescence signals, $\mathrm{OHF_{bg}}$ and $\mathrm{OHF_{tot}}$, and we refer to them as the background OH signal ($\mathrm{OH_{bg}}$) and the total OH signal ($\mathrm{OH_{tot}}$). The units of these variables are therefore molecules $\mathrm{cm^{-3}}$ OH equivalent and no inference is drawn as to the actual concentration of the interfering species.

The hyperbolic internal shape of IPI (max. cross section = 35 mm, min. cross section = 6 mm) (Fig. 3) is designed to minimize wall losses of OH and to provide rapid turbulent mixing of atmospheric air and added scavenger. A blower (SCL 20DH from FPZ, Italy) is directly connected to IPI pulling air with a flow rate between 140 and 280 $\mathrm{L\,min^{-1}}$. The flow velocity is monitored using a differential pressure sensor calibrated against a gas meter. A grid is located inside IPI below the inlet (Fig. 3, label 3) to create a homogenous flow profile within IPI. The OH scavenger is injected via eight 0.5 mm diameter holes (Fig. 3, label 1) into the centre of the flow of air sampled by IPI, 5 cm above the pinhole of the inlet (Fig. 3, label 2). Assuming plug flow, the estimated residence time of the ambient air in IPI from the injection of the scavenger to the instrument inlet when pulling 150 $\mathrm{L\,min^{-1}}$ of air, is ~ 4 ms. In order to improve the mixing between the scavenger and the sampled air, the injection happens at the minimum cross-section of IPI. In order to achieve a good penetration of the scavenger into the sample flow, the scavenger is injected into IPI with a carrier flow of synthetic air. The carrier air flow (~ 4000 sccm) is maintained at all times in order to keep the conditions in IPI constant. The HORUS inlet samples approximately 7 $\mathrm{L\,min^{-1}}$ of air directly from the centre of the flow.

There are several critical parameters involved in the deployment of this chemical scavenger methodology such as the identity and concentration of scavenger, the IPI sampling flow and therefore the residence time within IPI, and the synthetic air carrier flow. The choice of scavenger and concentration is very important. The OH scavenger must react quickly with OH but slowly with other oxidants like ozone and NO_3, it should not be toxic and not have a high absorptivity at the laser excitation wavelength. Its concentration should be high enough to effect the removal of a known and substantial proportion, $> 90\,\%$, of atmospheric OH but should not be in excess or there is a risk that excess scavenger will react with the internally generated OH. The flowrate of ambient air through IPI must be fast to minimize losses of HO_x (OH and HO_2) onto the walls and the residence time of OH within IPI has to be a good compromise between being short compared to the atmospheric lifetime of OH and allowing sufficient time for the scavenger to react. The carrier flow must be high enough to favour efficient mixing between the scavenger and the atmospheric air and to flush the lines when no injection of scavenger takes place. Figure 3 shows the schematic layout of the IPI during the HOPE 2012 campaign. The flow of the scavenger is controlled with a mass flow controller (MFC). After the MFC the scavenger line combines with the carrier gas line where it gets mixed. The mixture then reaches IPI where it is injected into the sampled atmospheric air. In both parts of the injection cycle, i.e. scavenger on and scavenger off, the same amount of air is sampled through IPI and the flow of carrier air is maintained constant. After the injection of the scavenger, the lines are flushed with synthetic air for approximately 5 s, to prevent remnants of the scavenger leaking into IPI during a scavenger off period. The current IPI cycle results in a minimum time resolution for the measurement of atmospheric OH of one data point over 4 min consisting of cycles of 2 min of injection of the OH scavenger and 2 min with no injection of the OH scavenger. Table 1 shows IPI parameters for three measurement campaigns. Details of the three measurement sites are given in the next section. During both HUMPPA-COPEC 2010 and DOMINO HO_x the prototype IPI version was in use. The main difference between the prototype version and the final design in current use, shown in Fig. 3, is the method of scavenger injection. The prototype IPI version injected the scavenger through eight 1/16 inch stainless steel tubes inserted into the centre of the IPI airstream. During these two campaigns the IPI parameters were the same. Propene (Aldrich 295663-330G, 99+% purity) was used as an OH scavenger with a flow of 20 sccm and was carried to IPI with 4000 sccm of synthetic air (Westfalen AG). Total IPI sample flow was $\sim 280\,\mathrm{L\,min^{-1}}$ leading to a concentration of propene of $6.4 \times 10^{14}\,\mathrm{molecules\,cm^{-3}}$. The residence time between the injection of the scavenger and the instrument inlet was ~ 2.5 ms, short compared to the lifetime of OH in those environments (on average ~ 80 ms) (Nölscher et al., 2012; Sinha et al., 2012). Under these conditions, more than 95 % of the atmospheric OH was scavenged within IPI. During HOPE 2012 the current version of IPI was used (Fig. 3). The current version was designed with a simplified layout to reduce the number of connections and improve ease of use. Two OH scavengers were tested during the campaign. The main scavenger used was propane (Air Liquide 3.5, 99.95 % purity) applied with an average flow of 17 sccm, a carrier flow of synthetic air of 4000 sccm and a sample flow within IPI of $\sim 150\,\mathrm{L\,min^{-1}}$ (propane concentration $\sim 2.5 \times 10^{15}\,\mathrm{molecules\,cm^{-3}}$). Pulling a smaller flow of atmospheric air through IPI led to a residence time after the injection of the scavenger of ~ 4 ms, that was still short compared to the average OH lifetime at the site (on average ~ 300 ms) and that allowed the use of a smaller concentration of scavenger preventing excessive titration of OH in the low pressure side of the instrument. With this concentration of propane, the lifetime of OH was 0.3 ms and a scavenging efficiency of ∼ 90 % was achieved. Propene was also used for some measurement cycles, for purposes of comparison, every few hours.

2.3 Measurement sites

We present measurements from three measurement sites represented by various meteorological and physicochemical characteristics. The HUMPPA-COPEC 2010 (Hyytiälä United Measurements of Photochemistry and Particles in Air – Comprehensive Organic Precursor Emission and Concentration study) campaign took place during the summer of 2010 at the SMEAR II station in Hyytiälä, Finland (61°51′ N, 24°17′ E, 181 m a.s.l.) in a boreal forest dominated by Scots Pine (*Pinus Silvestris* L.). Continuous measurements of several trace gases and meteorological parameters as well as particle size distribution and composition (Junninen, 2009) were available. For the first part of the campaign the HORUS instrument measured side-by-side with an OH CIMS operated by the University of Helsinki (Petäjä et al., 2009). The instrumentation and the meteorological conditions during the campaign are described by Williams et al. (2011). The DOMINO HO_x campaign took place in November 2010 in El Arenosillo, in south western Spain (37°1′ N, 6°7′ W, 40 m a.s.l.) at the same site as the DOMINO (Diel Oxidants Mechanisms In relation to Nitrogen Oxide) campaign in 2008 described in Crowley et al. (2011). The site is located in a forested area (Stone pines, *Pinus pinea*, 5–10 m in height) close to the South Atlantic Ocean shore and 12 km from the city of Huelva and the associated petrochemical industry. The HOPE 2012 (Hohenpeißenberg Photochemistry Experiment) campaign was conducted during the summer 2012 at the Meteorological Observatory in Hohenpeissenberg, Germany (47°48′ N, 11°2′ E). The observatory is operated by German Weather Service (DWD) and is located at an altitude of 985 m a.s.l. about 300 m above the surrounding terrain, which consists mainly of meadows and forests. During the entire campaign the HORUS instrument measured side-by-side with the OH CIMS operated by the German weather Service (DWD) (Berresheim et al., 2000). More information about the site and the routine measurements can be found in Handisides et al. (2003).

3 Results and discussion

3.1 IPI characterisation

The addition of IPI to HORUS has a significant effect on the performance of the instrument with respect to losses of radicals in the inlet system. In order to account for the perturbation on the measurement of atmospheric OH caused by the use of the IPI, a number of tests were completed to ascertain the effect of changing instrumental parameters. Total radical loss on the IPI system, the variation of this loss with the atmospheric air sampled and with scavenger carrier flow, and the efficiency of OH removal by the scavenger were tested during the different campaigns in which HORUS was in use with IPI. The tests described below were performed during the HOPE 2012 campaign with the current version of IPI (Fig. 3). Tests were performed during daytime, between 11:00 and 16:00 (LT), and nighttime after 20:00 (LT) in order to distinguish the effect of IPI in situations with high radical load, i.e. during the day, from situations where interferences might dominate the total signal, i.e. during the night.

Figure 4a and b show the average results of the radical loss tests checked by routinely measuring with and without IPI mounted on the inlet, conducted multiple times during the day and the night, respectively, with a sampled flow of $\sim 150\,\mathrm{L\,min^{-1}}$ and a carrier gas of 4000 sccm. The average total OH signal loss was 27 % during the day and 7 % during the night. Variability among data points during daytime tests was much larger than the equivalent tests during the night, most likely due to the high ambient variability of atmospheric OH and the lower variability of the background OH signal. Figure 4c shows the loss of the total OH signal with changing the sample flow through IPI with no carrier air and scavenger. The minimum loss, 20 %, occurs at sample flows larger than $500\,\mathrm{L\,min^{-1}}$ while at the flow in use during the campaign, $150\,\mathrm{L\,min^{-1}}$, the loss observed was ~ 30 %. Figure 4d shows the losses of the total OH signal in IPI with the variation of the additional carrier flow used to mix the scavenger with the sampled atmospheric air while sampling $150\,\mathrm{L\,min^{-1}}$ of air. No dependency on the dilution flow rate between 1000 and 5000 sccm and no additional loss of OH compared to the loss due to the sampling of 150 L min^{-1} of air were observed indicating that the major cause of losses is due to contact with surfaces. The measured losses during day time, on average 27 %, are the losses on the total OH signal and therefore the sum of the losses of atmospheric OH and losses of the species causing the background OH. During night time an average loss of 7 % was measured from the total OH signal; since the atmospheric OH signal was below the limit of detection of the instrument (4×10^5 molecules cm^{-3}, 4 min data) during the tests described, the loss is assumed to be entirely due to the species causing the background OH (L_{bg}). The loss of atmospheric OH (L_{OH}) is equal to the atmospheric OH signal measured with IPI mounted on the top of the inlet ($\mathrm{OH}^{\mathrm{IPI}}_{\mathrm{atm}}$) divided by the atmospheric OH signal measured without IPI mounted on the top of the inlet ($\mathrm{OH}^{\mathrm{NoIPI}}_{\mathrm{atm}}$).

$$L_{\mathrm{OH}} = \frac{\mathrm{OH}^{\mathrm{IPI}}_{\mathrm{atm}}}{\mathrm{OH}^{\mathrm{NoIPI}}_{\mathrm{atm}}} \tag{4}$$

The value of atmospheric OH without IPI mounted on the top of the inlet is impossible to measure but, by assuming that L_{bg} is constant, the loss on the atmospheric OH signal can be calculated using the equation below

$$L_{\mathrm{OH}} = \frac{\left(\mathrm{OH}^{\mathrm{IPI}}_{\mathrm{tot}} - \mathrm{OH}^{\mathrm{IPI}}_{\mathrm{bg}}\right)}{\mathrm{OH}^{\mathrm{NoIPI}}_{\mathrm{tot}} - \left(\frac{\mathrm{OH}^{\mathrm{IPI}}_{\mathrm{bg}}}{L_{\mathrm{bg}}}\right)} \tag{5}$$

$\mathrm{OH}^{\mathrm{IPI}}_{\mathrm{tot}}$ and $\mathrm{OH}^{\mathrm{IPI}}_{\mathrm{bg}}$ are the total OH signal and the background OH signal, respectively, measured by the instrument with IPI mounted on the inlet and therefore affected by losses and their difference is the atmospheric OH affected by losses, $\mathrm{OH}^{\mathrm{IPI}}_{\mathrm{atm}}$. $\mathrm{OH}^{\mathrm{NoIPI}}_{\mathrm{tot}}$ is the total OH signal measured during the tests without IPI on top of the inlet and therefore not affected by losses. The average value obtained for the loss of the atmospheric OH is 34 % and the data have been corrected accordingly. The variability observed for the average L_{OH} value, ±15 % (1σ), was taken into account for the accuracy of the HORUS instrument after the addition of IPI. The accuracy of HORUS was 34 % (2σ) and the accuracy of IPI-HORUS becomes 42 % (2σ).

To optimize the OH scavenging efficiency, several titrations of OH were conducted during the campaign with various operational conditions to examine the stability of the instrument and the reproducibility of the background subtraction. The optimization of the scavenger concentration is also important due to its potential to remove part of the internally produced OH in the low pressure region of the instrument, which would result in the overestimation of the atmospheric OH concentration. The titration experiments were performed by producing a constant above ambient concentration of OH in front of IPI using a mercury lamp and ambient air and by varying the concentration of the scavenger to measure the efficiency in the removal of the OH molecules within IPI. By sending a concentration of 2.5×10^{15} molecules cm^{-3} of propane, 90 % of the initial OH was removed. We calculated the theoretical scavenging efficiency for each OH scavenger deployed during the campaign based on the residence time in IPI after the injection of the scavenger ($\sim$ 4 ms) and inside the instrument in the low pressure region ($\sim$ 2.5 ms), and on the rate coefficients for the reactions between the respective scavenger and OH at ambient and low pressure ($\sim$ 350 Pa) (Sander et al., 2011). Figure 5 shows, in blue, the theoretical OH titration efficiency of scavenger depending on the scavenger concentration for the case of propane. Also shown are experimental titrations performed with propane, at different carrier gas flow rates. The carrier gas flow does not have a significant impact on the dilution of the scavenger as it represents only a minor percentage of the total flow sampled by IPI. What it does influence is the mixing of the scavenger with the atmospheric air, and thus the scavenging efficiency. The experimental data show a deviation from the calculated curve. At higher carrier gas flows the experimental data is closer to the model results. The deviation from the modelled data may be related to incomplete mixing between the sampled atmospheric air and the OH scavenger; by increasing the carrier gas flow, and therefore improving the mixing, we would expect to approach the theoretical titration efficiency. The set-up during the HOPE 2012 campaign allowed us to have a stable carrier flow only for flows below 4500 sccm. At higher values, the MFC controlling the carrier flow showed high sensitivity to even small temperature driven changes in the backing pressure of the supply gas. Therefore, the flow was kept stable at 4000 sccm, even though this is suboptimal with respect to mixing, and the amount of OH scavenged was checked regularly by repeated titrations. The calculated theoretical scavenging efficiency also predicts the amount of OH we would be removing in the low pressure region of the instrument at a certain concentration of scavenger. During the HOPE 2012 campaign the concentration of propane in use was small enough to allow the removal of less than 1 ‰ of the OH in the low pressure region.

The prototype IPI version was used during the HUMPPA-COPEC 2010 and the DOMINO HO_x campaigns and the instrument was run with the same parameters in both campaigns. Similar tests to the ones previously described were performed during HUMPPA-COPEC 2010 but as shown in Fig. 7, most of the total OH signal measured by the instrument was due to the background OH both during day and night time. In this situation, it is difficult to account for possible losses of the OH radical because its contribution on the total signal is too small. Total radical loss tests were performed but the results were not as unambiguous as for the HOPE 2012 campaign case; sometimes a small OH loss was observed on IPI but during most of the tests there was no clear indication of OH loss although any OH losses would likely be masked by the high background signal. Propene was originally selected as scavenger because of its high reaction rate with OH, allowing rapid OH scavenging even at low concentration. However, propene is known to form OH radicals after reaction with ozone with a yield of 0.34 (Atkinson et al., 2006). Hence, by mixing high concentrations of propene with the ambient air we expect formation of additional OH radicals. During HUMPPA-COPEC 2010 the residence time in IPI after the injection of the scavenger was ∼ 2.5 ms such that the concentration of ambient ozone and propene, even if reacting quickly with OH, can be assumed to be constant. The steady state concentration of OH with the concentration of propene within IPI ($\sim 6 \times 10^{14}$ molecules cm^{-3}) is reached after 0.5 ms, therefore the average steady state OH concentration produced by propene can be calculated by taking into account the average ambient ozone concentration during the campaign, the rate coefficient between ozone and propene, $k_1 = 1 \times 10^{-17}\,\mathrm{cm^3\,molecules^{-1}\,s^{-1}}$ at 298 K, the OH yield, $Y = 0.34$, and the rate coefficient between propene and OH at 1013 hPa and 298 K, $k_2 = 2.9 \times 10^{-11}\,\mathrm{cm^3\,molecules^{-1}\,s^{-1}}$ (Atkinson et al., 2006):

$$[\mathrm{OH}] = \frac{[\mathrm{O_3}] \times k_1 \times Y}{k_2} \qquad (6)$$

This calculation represents an upper limit for the possible production of OH during the injection of propene as scavenger as it does not consider any physical losses for OH or ozone on IPI and also assumes perfect mixing between propene and ambient air. The OH concentration produced during the injection of propene as scavenger depends only on the ozone concentration. The peak mixing ratio of ozone during the HUMPPA-COPEC 2010 campaign was 80 ppbv, which would result in a maximum OH concentration of 2.3×10^5 molecules cm^{-3}. For the average ozone value of 44 ppbv the steady state OH concentration would be 1.2×10^5 molecules cm^{-3}. This additional OH would cause an underestimation of the atmospheric OH calculated after subtraction of the background OH signal from the total OH measured by the instrument and would increase the uncertainty on our OH measurement. During the HOPE 2012 campaign we performed tests using propene and propane as OH scavengers intermittently at an ambient concentration of ozone of ∼ 40 ppbv to estimate the production of OH due to propene ozonolysis. Figure 6 shows the difference between the atmospheric OH concentration determined with the use of propane and the OH concentration determined using propene. The average difference observed was $(0.5 \pm 1.5) \times 10^5$ molecules cm^{-3} (1σ), lower than the theoretical value calculated for the same concentration of ozone indicating that additional loss processes likely happen. Because the ambient concentrations of ozone and the propene concentration in use during the tests performed in HOPE 2012 and HUMPPA-COPEC 2010 were comparable, assuming similar mixing within the two versions of IPI, we can expect similar OH production of 0.5×10^5 molecules cm^{-3} during the HUMPPA-COPEC 2010 campaign. The value is below the precision of the OH measurement and therefore the data were not corrected for this effect.

3.2 Atmospheric measurements using IPI

Figure 7 shows the signals resulting from the first use of HORUS with IPI during the HUMPPA-COPEC 2010 campaign. The top time series highlights the period in which the instrument was on the ground next to a CIMS measuring OH and H_2SO_4 (Petäjä et al., 2009), while the lower series shows the period in which the instrument was operated on a 24 m tower just above the forest canopy. During the day, within the partially shaded forest canopy, the background OH signal reaches up to 1×10^7 molecules cm^{-3} contributing 80 % to the total signal. On the tower the maximum value reached by the background OH signal is 7×10^6 molecules cm^{-3} contributing up to 60 % to the total OH signal measured on the majority of days. During night time the background OH concentration falls below 4×10^6 molecules cm^{-3}, but as the atmospheric OH concentration is small the fraction is almost 100 %. A side-by-side comparison with the CIMS instrument was performed for the first part of the campaign while both instruments were on the ground. Figure 8 shows the relationship between the atmospheric OH measured by the LIF and the OH measured by the CIMS. The correlation coefficient, $R^2 = 0.4$, is affected by the large scatter of the LIF OH data due to low laser power, a rapidly ageing detector, and the large contribution that the background signal makes to the total signal. Overall, the LIF measures higher OH values with a comparison slope of 1.40, however the difference is within the accuracy of the instruments (HORUS: 42 %, 2σ; CIMS: 64 %, 2σ) (Hens et al., 2013).

During the DOMINO HO_x campaign in November 2010 (Fig. 9), the background OH signal is always below 4×10^6 molecules cm^{-3} contributing about 50 % to the total OH measured during the day and 100 % during the night. During the three days of measurements, two different wind sectors were sampled; air travelling from the city of Huelva and air travelling over the continent. There appears to be little difference between the contributions of the background signal in either of these wind sectors.

Figure 10 shows the OH signals measured by HORUS during the HOPE 2012 campaign for a day at the beginning of the campaign (Fig. 10a) and a day at the end of the campaign (Fig. 10b). The data shown are representative of the concentrations generally observed during the campaign period. During the whole campaign the HORUS LIF was measuring side-by-side with a CIMS instrument (DWD-CIMS). The agreement between the two measurements of atmospheric OH is good, (Fig. 11), with a correlation coefficient for the entire data set of $R^2 = 0.81$, a slope of 0.94 and an offset of 4.5×10^5 molecules cm^{-3}. The offset is mainly caused by night time atmospheric OH observed during several nights by the HORUS instrument. This night time atmospheric OH is the signal remaining after the subtraction of the background OH signal from the total OH one and therefore is the atmospheric OH scavenged away by propane. The background OH signal during the campaign ranged from a minimum of 1×10^6 to a maximum of 7×10^6 molecules cm^{-3} on two days during which forest cutting was performed near the site but it was, for the most part, below 4×10^6 molecules cm^{-3}. The background signal contributed between 20 % and 40 % to the total OH signal during daytime and up to 100 % of the total OH signal during night time.

The three measurement campaigns show large differences in the background OH signal and its contribution to the total OH signal measured by HORUS. The smallest contribution to the total OH was observed during HOPE 2012, where the total OH measured by HORUS during day time for most of the days would have agreed with the DWD-CIMS instrument within the accuracy of the instruments even without the chemical scavenger method. At the other extreme lies the HUMPPA-COPEC 2010 campaign where the background OH signal within the forest canopy reaches 1×10^7 molecules cm^{-3} on top of a smaller atmospheric OH concentration, often below 2×10^6 molecules cm^{-3}. The relative contribution of the background signal is lower for the measurement period on the tower where the atmospheric concentration of OH is higher due to larger values of $J_{O(^1D)}$ compared to the location below the canopy (Hens et al., 2013). One difference between the conditions in HOPE 2012 and HUMPPA-COPEC 2010 is the measured OH reactivity, which was relatively high during HUMPPA-COPEC 2010, on average 12 s^{-1} with peaks of over 40 s^{-1} (Nölscher et al., 2012) and often below the detection limit during HOPE 2012 (on average 3.5±2 s^{-1}). The average concentration of measured BVOCs (isoprene, α-pinene, β-pinene, 3-carene, myrcene, sabinene) is similar for the two campaigns; approximately 300 pptv (Hens et al., 2013) with HUMPPA-COPEC 2010 showing high concentrations of monoterpenes and large emissions rates of sesquiterpenes (Yassaa et al., 2012) in addition to unexplained OH reactivity (Nölscher et al., 2012) that indicates the presence of unmeasured VOCs (Di Carlo et al., 2004). The interpretation of the DOMINO HO_x data is more complex; this campaign was at the same site of the DOMINO 2008 campaign but only a few trace gases (ozone and NO_x) and some meteorological parameters were measured in 2010. During the DOMINO 2008 campaign HORUS was in use without the injection of a chemical scavenger and due to the observation of an interfering signal during DOMINO HO_x, the OH concentration measured previously should be considered an upper limit. Because DOMINO HO_x was performed during the same month as the DOMINO 2008 campaign and no sign of differences in local pollution (street work, new buildings next to the site, etc.) or unusual weather was observed, we expect a similar amount of background OH, i.e. about 50 % of the total OH measured in DOMINO HO_x, for the DOMINO 2008 campaign. During DOMINO 2008 relatively high OH reactivity was measured, with an average of approximately 18 s^{-1} (Sinha et al., 2012), as well as low concentrations of measured BVOCs (mainly isoprene, eucalyptol and camphor) consistent with low emissions from vegetation due to the season, in the range of 50 pptv (Song et al., 2011) with isoprene being the most abundant BVOC measured. The concentration of anthropogenic VOCs (AVOCs) measured was on average 400 pptv consisting mainly of benzene and toluene, although only a fraction of the AVOCs were quantified on this campaign. The highest reactivity was found for air masses arriving from the continental sector due to the likely presence of reactive oxidation products formed from primary anthropogenic emissions, followed by the air coming from the Huelva sector because of the load of AVOCs (Sinha et al., 2012). As shown in Fig. 8, there is no clear difference between the background OH contributions to the total OH signal for the air arriving from those two different wind sectors indicating a similar influence on the background OH signal and a small contribution when compared to the OH background observed during the HUMPPA-COPEC 2010 where the measured BVOC concentrations were higher.

In summary, when the instrument was located within the canopy of a monoterpene dominated forest environment with high BVOC concentrations and high OH reactivity, the OH measurements with HORUS was strongly affected by an interference resulting in a high background OH signal. Aged air masses containing oxidation products from anthropogenic emissions and primary AVOCs such as benzene and toluene measured in high concentrations during DOMINO 2008 seem to contribute to a smaller background OH signal. The HUMPPA-COPEC 2010 campaign was an extreme case where most of the total OH measured by the instrument was due to the background OH signal, in part because of the large background, but also because the atmospheric OH concentration was low. In contrast, during DOMINO HO_x the total OH signal was not completely dominated by the contribution from the background signal even though the atmospheric OH concentration is comparable to that observed during HUMPPA-COPEC 2010. During HOPE 2012, a higher OH concentration in combination with a relatively low background OH signal, comparable to that in DOMINO HO_x, makes the contribution of the background OH to the total OH small during daytime. It is also evident that for all three measurement campaigns performed with IPI nearly the entire nocturnal OH signal detected is due to the background OH in the instrument and not due to atmospheric OH.

4 Possible influence on earlier measurements

The background OH signal is not a constant signal relating only to instrumental parameters. The signal depends on the type of environment and appears to be strongly related to the VOC concentration and type of VOC prevalent. It is possible that previous campaigns performed with LIF instruments without applying a chemical scavenger method have been affected by an interfering species in a similar manner as described in this manuscript. However, as underlined previously by Mao et al. (2012), the design of each particular LIF-FAGE system is likely to determine whether, and to what extent, the instrument suffers from this interference and so we will confine this discussion to the HORUS instrument.

The environment of previous campaigns may give an indication as to whether the measured OH was affected by significant inferences. The first campaign with HORUS consisted of a formal blind comparison, HOxCOMP, between several LIFs, a CIMS and a DOAS instrument both in a chamber and in ambient air. The results of the campaign are comprehensively described in Schlosser et al. (2009). In the daytime, the agreement between all the instruments in the chamber was good with a regression slope between the MPI LIF and the FZJ-DOAS of one, but in ambient air the MPI LIF instrument measured higher concentrations of OH than the CIMS (Schlosser et al., 2009). As we noticed an unattributed change in the calibration factor of the instrument of 30 %, we cannot exclude a change in the same order of magnitude in the calibration source between the period in the chamber and in ambient that might explain the difference between the OH concentration measured by the MPI LIF and the one measured by the CIMS in ambient air. Night time data from HORUS are not shown neither from the chamber period nor in ambient air because of large unexplained measured OH signals up to 4×10^{6} molecules cm^{-3} (Kubistin, 2009). Based on what we have learned since the use of IPI, it is likely that the high night time signal was due to a chemical interference in the HORUS instrument, however during day time its concentration appeared to be low enough in that specific environment, as to not produce a significant OH interference (i.e. within the accuracy of the instrument). Two subsequent campaigns, using HORUS, were performed without IPI. GABRIEL, an aircraft based campaign, took place in October 2005 over the tropical rain forest in equatorial South America (Kubistin et al., 2010). Measured OH was much higher than predicted by a traditional chemical mechanism. Further analysis indicated that OH might be recycled within the isoprene degradation scheme, not accounted so far in the traditional mechanism (Lelieveld et al., 2008; Kubistin et al., 2010; Taraborrelli et al., 2012). Although without IPI we cannot completely rule out a possible interference for our measurements, laboratory tests and quantum mechanical calculation as follow up studies to GABRIEL provided evidence for the proposed OH recycling, which was previously not accounted for (Dillon and Crowley, 2008; da Silva, 2010a; Peeters and Müller, 2010; Crounse et al., 2011). Measurements with a different LIF-FAGE instrument in the Borneo rainforest during the OP3 campaign (Whalley et al., 2011) also showed large discrepancies between measured and modelled OH using the traditional chemical mechanism. A side by side airborne comparison between the aircraft configuration of the GTHOS LIF instrument (ATHOS – Airborne Tropospheric Hydrogen Oxides Sensor) employed without a chemical scavenger method and a CIMS (Ren et al., 2012), showed good agreement even at higher levels of isoprene. This suggests that the background OH, observed by HORUS during HUMPPA-COPEC 2010, DOMINO HO_x and HOPE 2012, might be related to a shorter-lived species than isoprene that likely do not have a significant impact on aircraft measurements due to the relatively large distance between the emission source and the measurement point.

In addition, HOOVER, an airborne campaign in the upper troposphere across Europe in September 2007 (Regelin et al., 2013) which also did not employ the IPI system, showed good agreement between the measured OH and a simple box model suggesting that the OH LIF system was not adversely affected by background OH during this campaign.

5 Conclusions

An improved methodology to measure the OH radical with a LIF-FAGE instrument has been developed and deployed in three different environments. Results show that the use of the IPI-LIF-FAGE technique for HORUS results in good agreement with OH data measured with two different CIMS instruments during two campaigns. A thorough and careful characterisation of the optimal operational conditions was necessary in order to find the optimum tractable conditions to avoid inefficient mixing of the scavenger and the sampled air, excessive titration of OH in the low pressure side of the instrument, and large losses of OH on the walls of IPI. The best results were achieved when using propane as OH scavenger in a concentration of 2.5×10^{15} molecules cm^{-3} with a carrier gas flow of at least 6000 sccm and a residence time after the injection of the scavenger of ~ 4 ms. The use of a chemical scavenger method revealed the presence of a background OH signal that, using the same calibration factor as for atmospheric OH, spanned a concentration of 5×10^{5} to 1×10^{7} molecules cm^{-3} in the environments described. Without the chemical scavenger method the atmospheric OH measured during the HUMPPA-COPEC 2010, DOMINO HO_x and HOPE 2012 campaigns, during day and night time, would have been overestimated. Further investigations into the origin and cause of such a background OH signal will be the subject of ongoing work though it is already clear that the background OH has a strong connection with the type of environment in which the instrument is deployed. Although it is very likely that the presence and extent of a chemical interference in different LIF-FAGE systems for the measurement of OH are dependent on the particular instrument design, our experiences show that the determination of the background OH should be a prerequisite for these systems and the ambient measurement of OH.

Acknowledgements. Work during HUMPPA-COPEC was supported by the Hyytiälä site engineers and staff. Support of the European Community Research Infrastructure Action under the FP6 "Structuring the European Research Area" Programme, EUSAAR Contract No RII3-CT-2006-026140 is gratefully acknowledged. The HUMPPA-COPEC 2010 campaign measurements and analyses were supported by the ERC Grant ATMNUCLE (project No 227463), Academy of Finland Centre of Excellence program (project No 1118615), the European integrated project on Aerosol Cloud Climate and Air Quality Interactions EUCAARI (project No 036833-2), the EUSAAR TNA (project No 400586), and the IMECC TA (project No 4006261).

The work during HOPE 2012 was supported by the scientists and staff of DWD Hohenpeißenberg whom we would like to thank for providing the "platform" and opportunity to perform such campaigns devoted to a better process understanding of atmospheric chemistry. In particular, we thank Anja Werner, Jennifer Englert and Katja Michl for the VOC measurements, Stephan Gilge for the trace gases measurements and Georg Stange for running the CIMS.

We also would like to thank Gavin Phillips of the Department of Atmospheric Chemistry, MPIC for useful discussions and for assistance with the manuscript and Markus Rudolf for much technical support and guidance.

The service charges for this open access publication
have been covered by the Max Planck Society.

References

Atkinson, R., Baulch, D. L., Cox, R. A., Crowley, J. N., Hampson, R. F., Hynes, R. G., Jenkin, M. E., Rossi, M. J., Troe, J., and IUPAC Subcommittee: Evaluated kinetic and photochemical data for atmospheric chemistry: Volume II – gas phase reactions of organic species, Atmos. Chem. Phys., 6, 3625–4055, doi:10.5194/acp-6-3625-2006, 2006.

Berresheim, H., Elste, T., Plass-Dülmer, C., Eisele, F. L., and Tanner, D. J.: Chemical ionization mass spectrometer for long-term measurements of atmospheric OH and H_2SO_4, Int. J. Mass Spectrom., 202, 91–109, 2000.

Crounse, J. D., Paulot, F., Kjaergaard, H. G., and Wennberg, P. O.: Peroxy radical isomerization in the oxidation of isoprene, Phys. Chem. Chem. Phys., 13, 13607–13613, 2011.

Crowley, J. N., Thieser, J., Tang, M. J., Schuster, G., Bozem, H., Beygi, Z. H., Fischer, H., Diesch, J.-M., Drewnick, F., Borrmann, S., Song, W., Yassaa, N., Williams, J., Pöhler, D., Platt, U., and Lelieveld, J.: Variable lifetimes and loss mechanisms for NO_3 and N_2O_5 during the DOMINO campaign: contrasts between marine, urban and continental air, Atmos. Chem. Phys., 11, 10853–10870, doi:10.5194/acp-11-10853-2011, 2011.

da Silva, G.: Hydroxyl radical regeneration in the photochemical oxidation of glyoxal: kinetics and mechanism of the $HC(O)CO + O_2$ reaction, Phys. Chem. Chem. Phys., 12, 6698–6705, 2010a.

da Silva, G.: Kinetics and mechanism of the glyoxal + HO_2 reaction: conversion of HO_2 to OH by carbonyls, J. Phys. Chem. A, 115, 291–297, 2010b.

da Silva, G.: Oxidation of carboxylic acids regenerates hydroxyl radicals in the unpolluted and nighttime troposphere, J. Phys. Chem. A, 114, 6861–6869, 2010c.

Di Carlo, P., Brune, W. H., Martinez, M., Harder, H., Lesher, R., Ren, X. R., Thornberry, T., Carroll, M. A., Young, V., Shepson, P. B., Riemer, D., Apel, E., and Campbell, C.: Missing OH reactivity in a forest: evidence for unknown reactive biogenic VOCs, Science, 304, 722–725, 2004.

Dillon, T. J. and Crowley, J. N.: Direct detection of OH formation in the reactions of HO_2 with $CH_3C(O)O_2$ and other substituted peroxy radicals, Atmos. Chem. Phys., 8, 4877–4889, doi:10.5194/acp-8-4877-2008, 2008.

Eisele, F. L. and Tanner, D. J.: Ion-assisted tropospheric OH measurements, J. Geophys. Res.-Atmos., 96, 9295–9308, 1991.

Eisele, F. L., Mauldin, R. L., Tanner, D. J., Cantrell, C., Kosciuch, E., Nowak, J. B., Brune, B., Faloona, I., Tan, D., Davis, D. D., Wang, L., and Chen, G.: Relationship between OH measurements on two different NASA aircraft during PEM Tropics B, J. Geophys. Res.-Atmos., 106, 32683–32689, 2001.

Faloona, I., Tan, D., Brune, W., Hurst, J., Barket, D., Couch, T. L., Shepson, P., Apel, E., Riemer, D., Thornberry, T., Carroll, M. A., Sillman, S., Keeler, G. J., Sagady, J., Hooper, D., and Paterson, K.: Nighttime observations of anomalously high levels of hydroxyl radicals above a deciduous forest canopy, J. Geophys. Res.-Atmos., 106, 24315–24333, 2001.

Faloona, I., Tan, D., Lesher, R., Hazen, N., Frame, C., Simpas, J., Harder, H., Martinez, M., Di Carlo, P., Ren, X., and Brune, W.: A laser-induced fluorescence instrument for detecting tropospheric OH and HO_2: characteristics and calibration, J. Atmos. Chem., 47, 139–167, 2004.

Handisides, G. M., Plass-Dülmer, C., Gilge, S., Bingemer, H., and Berresheim, H.: Hohenpeissenberg Photochemical Experiment (HOPE 2000): measurements and photostationary state calculations of OH and peroxy radicals, Atmos. Chem. Phys., 3, 1565–1588, doi:10.5194/acp-3-1565-2003, 2003.

Hard, T. M., O'Brien, R. J., Chan, C. Y., and Mehrabzadeh, A. A.: Tropospheric free radical determination by fluorescence assay with gas expansion, Environ. Sci. Technol., 18, 768–777, 1984.

Hens, K., Novelli, A., Martinez, M., Auld, J., Axinte, R., Bohn, B., Fischer, H., Keronen, P., Kubistin, D., Nölscher, A. C., Oswald, R., Paasonen, P., Petäjä, T., Regelin, E., Sander, R., Sinha, V., Sipilä, M., Taraborrelli, D., Tatum Ernest, C., Williams, J., Lelieveld, J., and

Harder, H.: Observation and modelling of HO_x radicals in a boreal forest, Atmos. Chem. Phys. Discuss., 13, 28561–28629, doi:10.5194/acpd-13-28561-2013, 2013.

Hofzumahaus, A., Aschmutat, U., Brandenburger, U., Brauers, T., Dorn, H. P., Hausmann, M., Heßling, M., Holland, F., Plass-Dülmer, C., and Ehhalt, D. H.: Intercomparison of tropospheric OH measurements by different laser techniques during the POPCORN Campaign 1994, J. Atmos. Chem., 31, 227–246, 1998.

Hofzumahaus, A., Rohrer, F., Lu, K., Bohn, B., Brauers, T., Chang, C.-C., Fuchs, H., Holland, F., Kita, K., Kondo, Y., Li, X., Lou, S., Shao, M., Zeng, L., Wahner, A., and Zhang, Y.: Amplified trace gas removal in the troposphere, Science, 324, 1702–1704, 2009.

Holland, F. and Hessling, M.: In situ measurement of tropospheric OH radicals by laser-induced fluorescence, J. Atmos. Sci., 52, 3393–3401, 1995.

Junninen, H. L. A., Keronen, P., Aalto, P., Hiltunen, V., Hari, P., and Kulmala, M.: Smart-SMEAR: on-line data exploration and visualization tool for SMEAR stations, Boreal Env. Res., 14, 447–457, 2009.

Kubistin, D.: OH und HO_2 Radikale uber dem tropischen Regenwald, 2009, Physics, Johannes Gutenberg Univeristät, Germany, Mainz, 2009.

Kubistin, D., Harder, H., Martinez, M., Rudolf, M., Sander, R., Bozem, H., Eerdekens, G., Fischer, H., Gurk, C., Klüpfel, T., Königstedt, R., Parchatka, U., Schiller, C. L., Stickler, A., Taraborrelli, D., Williams, J., and Lelieveld, J.: Hydroxyl radicals in the tropical troposphere over the Suriname rainforest: comparison of measurements with the box model MECCA, Atmos. Chem. Phys., 10, 9705–9728, doi:10.5194/acp-10-9705-2010, 2010.

Lelieveld, J., Butler, T. M., Crowley, J. N., Dillon, T. J., Fischer, H., Ganzeveld, L., Harder, H., Lawrence, M. G., Martinez, M., Taraborrelli, D., and Williams, J.: Atmospheric oxidation capacity sustained by a tropical forest, Nature, 452, 737–740, 2008.

Levy, H.: Normal atmosphere – large radical and formaldehyde concentrations predicted, Science, 173, 141–143, 1971.

Levy, H.: Photochemistry of the troposphere, in: Advances in Photochemistry, John Wiley & Sons, Inc., 1974.

Mao, J., Ren, X., Zhang, L., Van Duin, D. M., Cohen, R. C., Park, J.-H., Goldstein, A. H., Paulot, F., Beaver, M. R., Crounse, J. D., Wennberg, P. O., DiGangi, J. P., Henry, S. B., Keutsch, F. N., Park, C., Schade, G. W., Wolfe, G. M., Thornton, J. A., and Brune, W. H.: Insights into hydroxyl measurements and atmospheric oxidation in a California forest, Atmos. Chem. Phys., 12, 8009–8020, doi:10.5194/acp-12-8009-2012, 2012.

Martinez, M., Harder, H., Ren, X., Lesher, R. L., and Brune, W. H.: Measuring atmospheric naphthalene with laser-induced fluorescence, Atmos. Chem. Phys., 4, 563–569, doi:10.5194/acp-4-563-2004, 2004.

Martinez, M., Harder, H., Kubistin, D., Rudolf, M., Bozem, H., Eerdekens, G., Fischer, H., Klüpfel, T., Gurk, C., Königstedt, R., Parchatka, U., Schiller, C. L., Stickler, A., Williams, J., and Lelieveld, J.: Hydroxyl radicals in the tropical troposphere over the Suriname rainforest: airborne measurements, Atmos. Chem. Phys., 10, 3759–3773, doi:10.5194/acp-10-3759-2010, 2010.

Nölscher, A. C., Williams, J., Sinha, V., Custer, T., Song, W., Johnson, A. M., Axinte, R., Bozem, H., Fischer, H., Pouvesle, N., Phillips, G., Crowley, J. N., Rantala, P., Rinne, J., Kulmala, M., Gonzales, D., Valverde-Canossa, J., Vogel, A., Hoffmann, T., Ouwersloot, H. G., Vilà-Guerau de Arellano, J., and Lelieveld, J.: Summertime total OH reactivity measurements from boreal forest during HUMPPA-COPEC 2010, Atmos. Chem. Phys., 12, 8257–8270, doi:10.5194/acp-12-8257-2012, 2012.

Peeters, J. and Müller, J.-F.: HO_x radical regeneration in isoprene oxidation via peroxy radical isomerisations. II: experimental evidence and global impact, Phys. Chem. Chem. Phys., 12, 14227–14235, 2010.

Peeters, J., Nguyen, T. L., and Vereecken, L.: HO_x radical regeneration in the oxidation of isoprene, Phys. Chem. Chem. Phys., 11, 5935–5939, 2009.

Perner, D., Platt, U., Trainer, M., Hübler, G., Drummond, J., Junkermann, W., Rudolph, J., Schubert, B., Volz, A., Ehhalt, D. H., Rumpel, K. J., and Helas, G.: Measurements of tropospheric OH concentrations: a comparison of field data with model predictions, J. Atmos. Chem., 5, 185–216, 1987.

Petäjä, T., Mauldin, III, R. L., Kosciuch, E., McGrath, J., Nieminen, T., Paasonen, P., Boy, M., Adamov, A., Kotiaho, T., and Kulmala, M.: Sulfuric acid and OH concentrations in a boreal forest site, Atmos. Chem. Phys., 9, 7435–7448, doi:10.5194/acp-9-7435-2009, 2009.

Regelin, E., Harder, H., Martinez, M., Kubistin, D., Tatum Ernest, C., Bozem, H., Klippel, T., Hosaynali-Beygi, Z., Fischer, H., Sander, R., Jöckel, P., Königstedt, R., and Lelieveld, J.: HO_x measurements in the summertime upper troposphere over Europe: a comparison of observations to a box model and a 3-D model, Atmos. Chem. Phys., 13, 10703–10720, doi:10.5194/acp-13-10703-2013, 2013.

Ren, X., Harder, H., Martinez, M., Faloona, I., Tan, D., Lesher, R., Di Carlo, P., Simpas, J., and Brune, W.: Interference testing for atmospheric HO_x measurements by laser-induced fluorescence, J. Atmos. Chem., 47, 169–190, 2004.

Ren, X., Olson, J. R., Crawford, J. H., Brune, W. H., Mao, J., Long, R. B., Chen, Z., Chen, G., Avery, M. A., Sachse, G. W., Barrick, J. D., Diskin, G. S., Huey, L. G., Fried, A., Cohen, R. C., Heikes, B., Wennberg, P. O., Singh, H. B., Blake, D. R., and Shetter, R. E.: HO_x chemistry during INTEX-A 2004: Observation, model calculation, and comparison with previous studies, J. Geophys. Res.-Atmos., 113, D05310, doi:10.1029/2007JD009166, 2008.

Ren, X., Mao, J., Brune, W. H., Cantrell, C. A., Mauldin III, R. L., Hornbrook, R. S., Kosciuch, E., Olson, J. R., Crawford, J. H., Chen, G., and Singh, H. B.: Airborne intercomparison of HO_x measurements using laser-induced fluorescence and chemical ionization mass spectrometry during ARCTAS, Atmos. Meas. Tech., 5, 2025–2037, doi:10.5194/amt-5-2025-2012, 2012.

Sander, S. P., Abbatt, J., Barker, J. R., Burkholder, J. B., Friedl, R. R., Golden, D. M., Huie, R. E., Kolb, C. E., Kurylo, M. J., Moortgat, G. K., Orkin, V. L., and Wine, P. H.: Chemical Kinetics and Photochemical Data for Use in Atmospheric Studies, Evaluation No. 17, JPL Publication 10-6 Jet Propulsion Laboratory Pasadena, California, 2011, 2011.

Schlosser, E., Bohn, B., Brauers, T., Dorn, H.-P., Fuchs, H., Häseler, R., Hofzumahaus, A., Holland, F., Rohrer, F., Rupp, L., Siese, M., Tillmann, R., and Wahner, A.: Intercomparison of two hydroxyl radical measurement techniques at the atmosphere simulation chamber SAPHIR, J. Atmos. Chem., 56, 187–205, 2007.

Schlosser, E., Brauers, T., Dorn, H.-P., Fuchs, H., Häseler, R., Hofzumahaus, A., Holland, F., Wahner, A., Kanaya, Y., Kajii, Y., Miyamoto, K., Nishida, S., Watanabe, K., Yoshino, A., Kubistin, D., Martinez, M., Rudolf, M., Harder, H., Berresheim, H., Elste, T., Plass-Dülmer, C., Stange, G., and Schurath, U.: Technical Note: Formal blind intercomparison of OH measurements: results from the international campaign HOxComp, Atmos. Chem. Phys., 9, 7923–7948, doi:10.5194/acp-9-7923-2009, 2009.

Sinha, V., Williams, J., Diesch, J. M., Drewnick, F., Martinez, M., Harder, H., Regelin, E., Kubistin, D., Bozem, H., Hosaynali-Beygi, Z., Fischer, H., Andrés-Hernández, M. D., Kartal, D., Adame, J. A., and Lelieveld, J.: Constraints on instantaneous ozone production rates and regimes during DOMINO derived using in-situ OH reactivity measurements, Atmos. Chem. Phys., 12, 7269–7283, doi:10.5194/acp-12-7269-2012, 2012.

Song, W., Williams, J., Yassaa, N., Martinez, M., Carnero, J., Hidalgo, P., Bozem, H., and Lelieveld, J.: Winter and summer characterization of biogenic enantiomeric monoterpenes and anthropogenic BTEX compounds at a Mediterranean Stone Pine forest site, J. Atmos. Chem., 68, 233–250, 2011.

Taraborrelli, D., Lawrence, M. G., Crowley, J. N., Dillon, T. J., Gromov, S., Groß, C. B. M., Vereecken, L., and Lelieveld, J.: Hydroxyl radical buffered by isoprene oxidation over tropical forests, Nat. Geosci., 5, 190–193, 2012.

Wennberg, P. O., Cohen, R. C., Hazen, N. L., Lapson, L. B., Allen, N. T., Hanisco, T. F., Oliver, J. F., Lanham, N. W., Demusz, J. N., and Anderson, J. G.: Aircraft-borne, laser-induced fluorescence instrument for the in situ detection of hydroxyl and hydroperoxyl radicals, Rev. Sci. Instrum., 65, 1858–1876, 1994.

Whalley, L. K., Edwards, P. M., Furneaux, K. L., Goddard, A., Ingham, T., Evans, M. J., Stone, D., Hopkins, J. R., Jones, C. E., Karunaharan, A., Lee, J. D., Lewis, A. C., Monks, P. S., Moller, S. J., and Heard, D. E.: Quantifying the magnitude of a missing hydroxyl radical source in a tropical rainforest, Atmos. Chem. Phys., 11, 7223–7233, doi:10.5194/acp-11-7223-2011, 2011.

White, J. U.: Long optical paths of large aperture, J. Opt. Soc. Am., 32, 285–288, 1942.

Williams, J., Crowley, J., Fischer, H., Harder, H., Martinez, M., Petäjä, T., Rinne, J., Bäck, J., Boy, M., Dal Maso, M., Hakala, J., Kajos, M., Keronen, P., Rantala, P., Aalto, J., Aaltonen, H., Paatero, J., Vesala, T., Hakola, H., Levula, J., Pohja, T., Herrmann, F., Auld, J., Mesarchaki, E., Song, W., Yassaa, N., Nölscher, A., Johnson, A. M., Custer, T., Sinha, V., Thieser, J., Pouvesle, N., Taraborrelli, D., Tang, M. J., Bozem, H., Hosaynali-Beygi, Z., Axinte, R., Oswald, R., Novelli, A., Kubistin, D., Hens, K., Javed, U., Trawny, K., Breitenberger, C., Hidalgo, P. J., Ebben, C. J., Geiger, F. M., Corrigan, A. L., Russell, L. M., Ouwersloot, H. G., Vilà-Guerau de Arellano, J., Ganzeveld, L., Vogel, A., Beck, M., Bayerle, A., Kampf, C. J., Bertelmann, M., Köllner, F., Hoffmann, T., Valverde, J., González, D., Riekkola, M.-L., Kulmala, M., and Lelieveld, J.: The summertime Boreal forest field measurement intensive (HUMPPA-COPEC-2010): an overview of meteorological and chemical influences, Atmos. Chem. Phys., 11, 10599–10618, doi:10.5194/acp-11-10599-2011, 2011.

Yassaa, N., Song, W., Lelieveld, J., Vanhatalo, A., Bäck, J., and Williams, J.: Diel cycles of isoprenoids in the emissions of Norway spruce, four Scots pine chemotypes, and in Boreal forest ambient air during HUMPPA-COPEC-2010, Atmos. Chem. Phys., 12, 7215–7229, doi:10.5194/acp-12-7215-2012, 2012.

York, D., Evensen, N. M., Martìnez, M. L., and De Basabe Delgado, J.: Unified equations for the slope, intercept, and standard errors of the best straight line, Am. J. Phys., 72, 367–375, 2004.

Table 1. IPI parameters for the three measurement campaigns.

Campaign	IPI flow Residence time	Scavenger/Flow	Carrier flow (Syn. Air)	Measured scavenging efficiency
HUMPPA COPEC 2010 and DOMINO HO_x	$280\,L\,min^{-1}$ ~ 2.5 ms	Propene/20 sccm	4000 sccm	$> 95\,\%$
HOPE 2012	$150\,L\,min^{-1}$ ~ 4 ms	Propane/5–30 sccm Propene/2–8 sccm	2700–4300 sccm	60–95 %

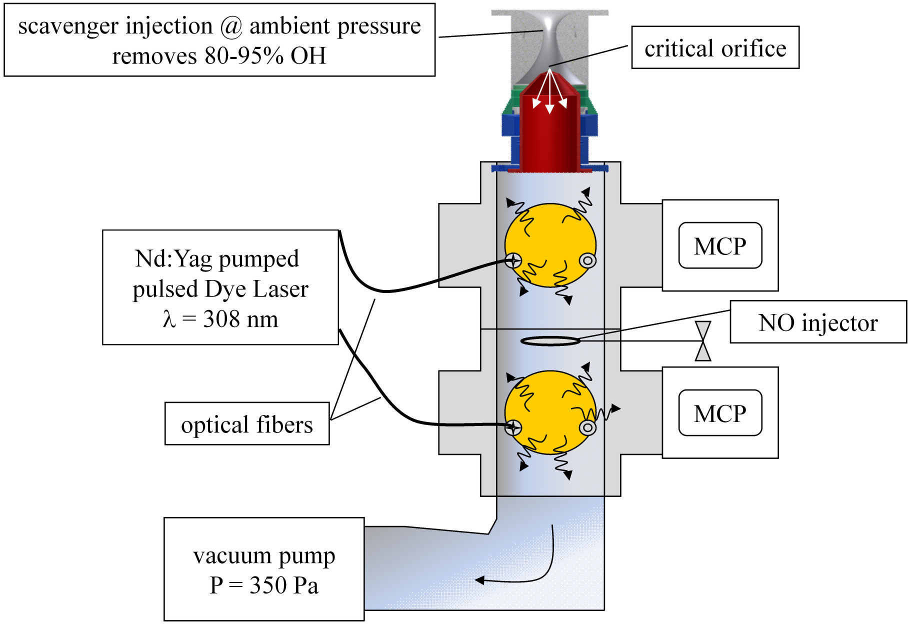

Fig. 1. HORUS instrument setup scheme with IPI. The ambient air is sampled through IPI where an OH scavenger is added periodically and is then sampled by the instrument inlet through a critical orifice. In the first cell, OH is excited by a laser pulse at around 308 nm and the fluorescence is detected by an MCP. Immediately before the second cell a mixture of NO with nitrogen is injected and HO_2 is detected after conversion into OH. The total pressure inside the instrument is maintained around 350 Pa.

Title Page
Abstract Introduction
Conclusions References
Tables Figures
◀| |▶
◀ ▶
Back Close
Full Screen / Esc
Printer-friendly Version
Interactive Discussion

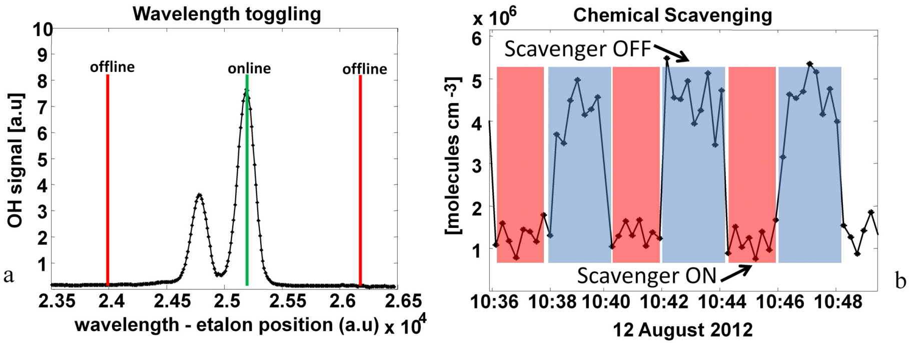

Fig. 2. **(a)** HORUS instrumental fluorescence background signal is detected by tuning the excitation laser on (green line) and off resonance (red lines) with the OH line at 308 nm; **(b)** the background OH signal is obtained by injecting an OH scavenger periodically in front of the inlet (red shaded area). The blue shaded area represents the total OH signal. The atmospheric OH is obtained from the difference between these two.

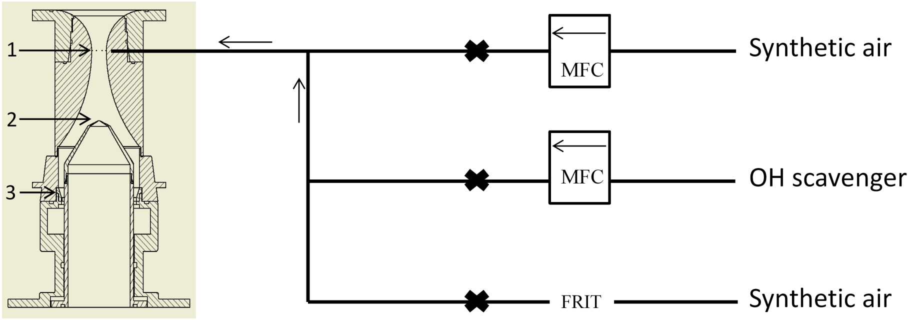

Fig. 3. Inlet pre injector (IPI) scheme. The injection of the scavenger is achieved via eight 0.5 mm holes (Label 1) positioned 5 cm above the pinhole of the inlet (Label 2). The scavenger is carried through IPI with ∼ 4000 sccm of synthetic air. The residence time in IPI after the injection of the scavenger is ∼ 4 ± 0.5 ms in order to scavenge between 80 % and 95 % of the atmospheric OH, depending on the scavenger concentration. Label 3 indicates the position of a metallic grid.

Title Page
Abstract
Introduction
Conclusions
References
Tables
Figures
◂◂
▸▸
◂
▸
Back
Close
Full Screen / Esc
Printer-friendly Version
Interactive Discussion

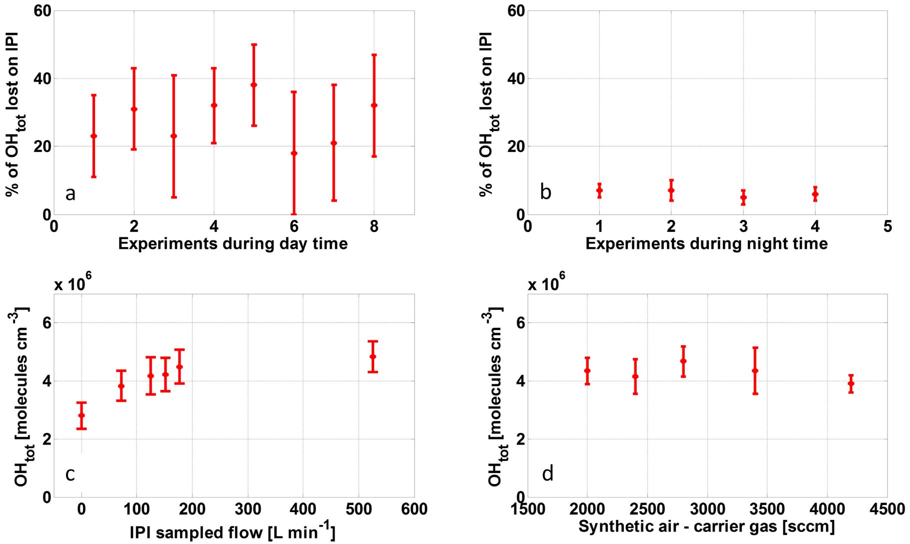

Fig. 4. **(a)** and **(b)** represent the losses of the total OH signal observed by measuring with and without IPI mounted on top of the inlet for day **(a)** and night **(b)** time; **(c)** total OH signal measured while varying the sample flow through IPI; **(d)** total OH signal measured with a constant IPI sampling flow of ~ 150 L min^{-1} and adding between 2000 and 4300 sccm of carrier gas flow.

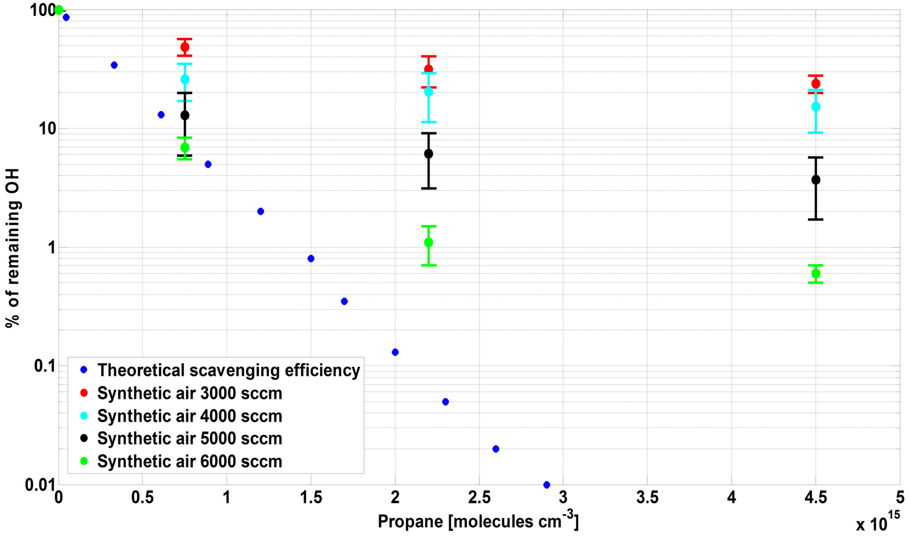

Fig. 5. Comparison between the calculated theoretical scavenging efficiency of propane and the measured scavenging efficiency at four different synthetic air carrier gas flows for three different concentrations of propane.

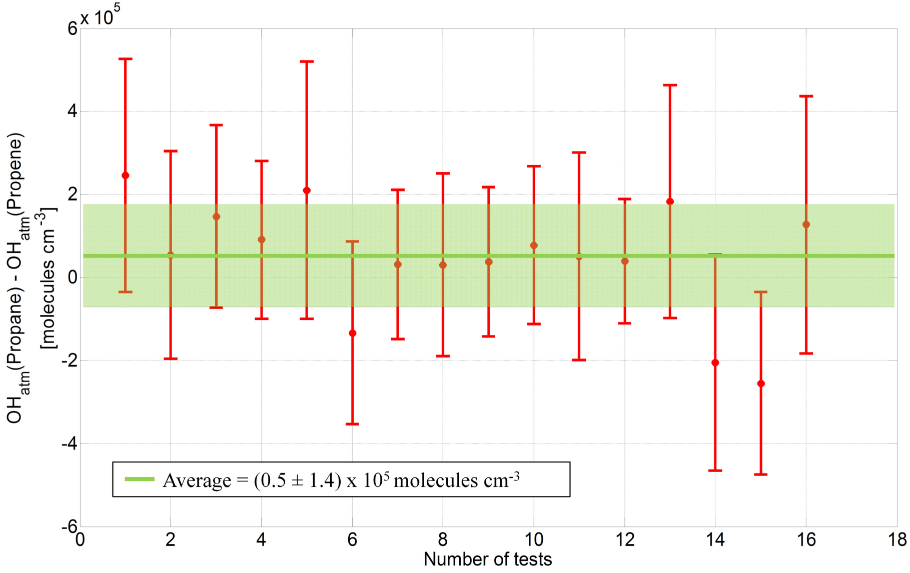

Fig. 6. Difference between the atmospheric OH concentration determined with the use of propane as scavenger and the atmopspheric OH concentration determined with the use of propene. The points are one hour averages. The green line is the average value of 0.5×10^5 molecules cm^{-3} and the shaded area is the 1σ range.

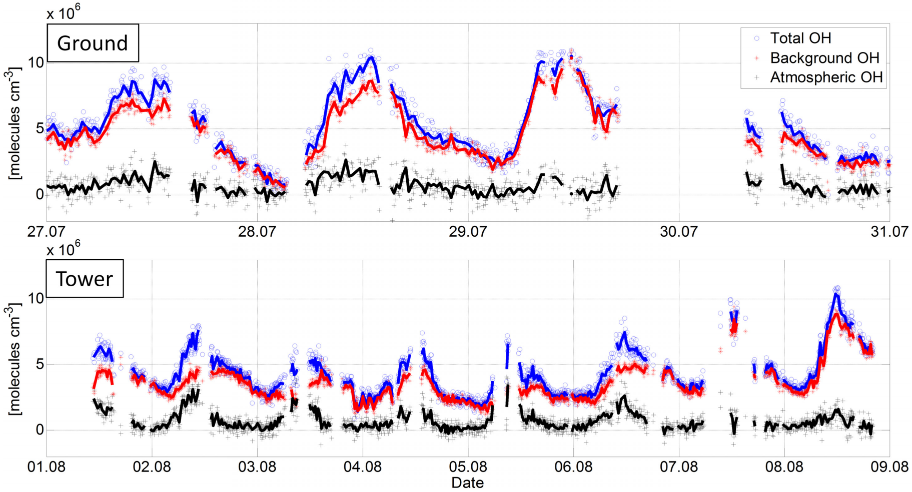

Fig. 7. OH signals measured by HORUS during HUMPPA-COPEC 2010 campaign. The blue circles represent the total OH signal measured by the instrument in the absence of an OH scavenger. The red stars represent the background OH measured during the injection of an OH scavenger. The black crosses represent the atmospheric OH obtained by difference between total OH and background OH. The solid lines are 30 min averages. The top panel shows the data collected on the ground and the bottom panel shows the data collected on the tower. Time is in UTC+2.

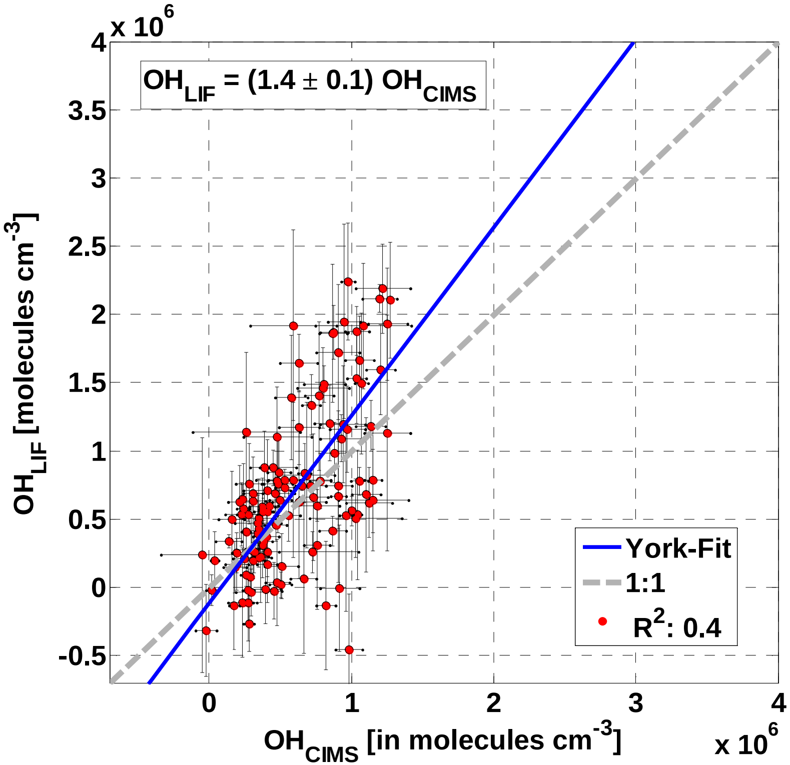

Fig. 8. Comparison of OH radical measurements by HORUS and CIMS instruments during the HUMPPA-COPEC 2010 campaign based on 30 min averages data. Linear regression following the method of York et al. (2004) yields a slope of 1.40 ± 0.1 and an offset of $(-1.2 \pm 0.3) \times 10^5$ molecules cm^{-3}. The precision on the atmospheric OH has been estimated based on the variability of the atmospheric OH signal within two hours and therefore represents an upper limit precision since it is partially influenced by the atmospheric variability of the ambient OH.

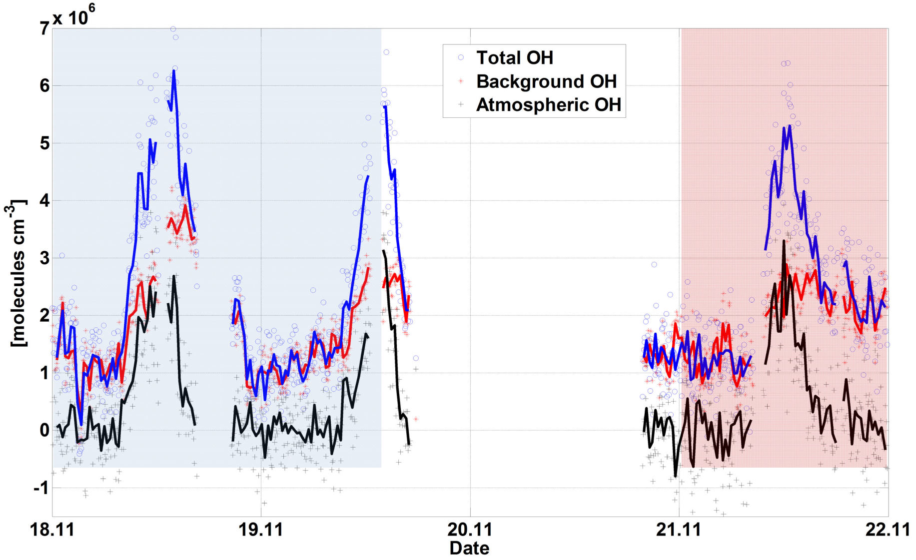

Fig. 9. OH signals measured by HORUS during the DOMINO HO_x campaign. The blue circles represent the total OH signal measured by the instrument in the absence of an OH scavenger. The red stars represent the background OH measured during the injection of an OH scavenger. The black crosses represent the atmospheric OH obtained by difference between total OH and background OH. The solid lines are 30 min averages. The two shaded areas represent the two prevailing wind directions: the blue area during wind from the continental sector and the red area from the Huelva sector. Time is in UTC.

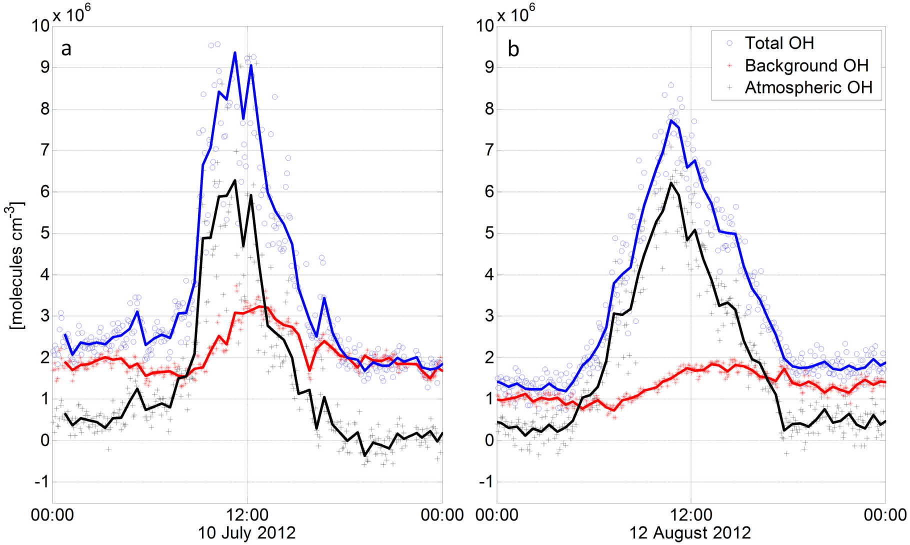

Fig. 10. OH signals measured by HORUS during the HOPE 2012 campaign for a day at the beginning **(a)** and at the end **(b)** of the campaign. The blue circles represent the total OH signal measured in the absence of an OH scavenger. The red stars represent the background OH measured during the injection of an OH scavenger. The black crosses represent the atmospheric OH obtained by difference between total OH and background OH. The solid lines are 30 min averages. Time is in UTC.

Title Page
Abstract | Introduction
Conclusions | References
Tables | Figures
◂◂ | ▸▸
◂ | ▸
Back | Close
Full Screen / Esc
Printer-friendly Version
Interactive Discussion

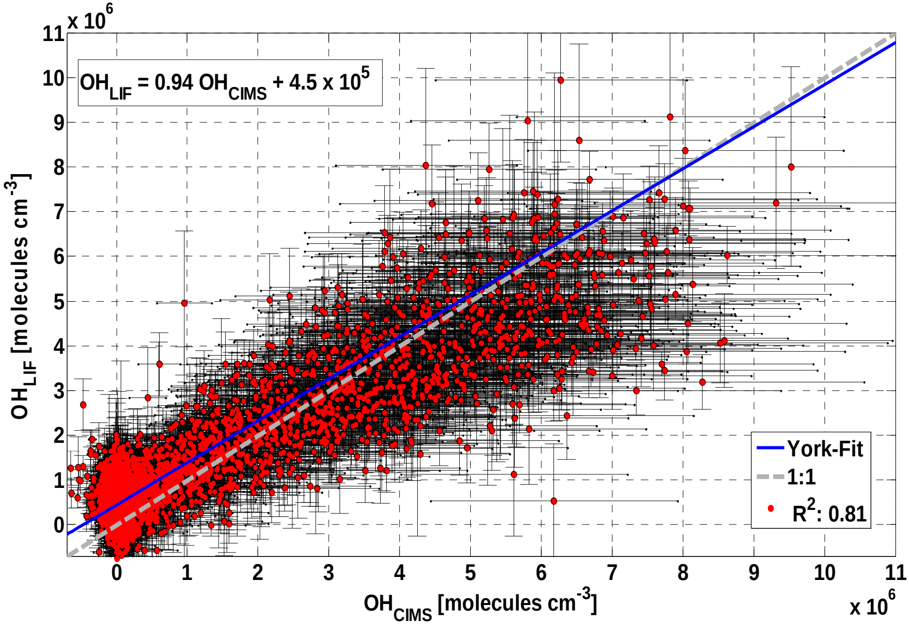

Fig. 11. Comparison of OH radical measurements by HORUS LIF and DWD-CIMS instruments during the HOPE 2012 campaign based on 4 min average data. The linear regression following the method by York et al. (2004) yields a slope of 0.94 ± 0.01 and an offset of $(4.5 \pm 0.06) \times 10^5$ molecules cm^{-3}.